ELSEVIER

Journal of Non-Crystalline Solids 192&193 (1995) 570–573

JOURNAL OF NON-CRYSTALLINE SOLIDS

Nanocrystallization of amorphous Co–Si–B alloys with strong compound forming additions

V. Stelmukh *, A. Gurov, L. Voropaeva, N. Novokhatskaya, A. Serebryakov

Solid State Physics Institute, Russian Academy of Sciences, Chernogolovka, Moscow District 142432, Russian Federation

Abstract

Nanoscale structures were found to form by the primary crystallization of Co–Si–B amorphous alloys with Nb and Hf additions. The results of a transmission electron microscopy and X-ray diffraction study of the nanocrystalline structures formed on short-time and conventional furnace annealing in a wide temperature range are presented. The origin of the observed alloying effect is briefly discussed.

1. Introduction

Nanocrystallization of amorphous metallic alloys has become of great interest since 1988 when Yoshizawa et al. [1] reported on new soft ferromagnets denoted as 'finemets' (FMs). The FMs were prepared by crystallization of Fe-based amorphous alloys. They have extremely fine grains and exhibit superior magnetic properties.

It is now well recognized that alloying elements play a key role in the formation of nanocrystals in metallic glasses (e.g., Refs. [2–6]). However, it is not yet fully understood why some alloying elements facilitate nanocrystallization, whereas others do not. The main difficulty in discerning the nature of the observed alloying effects is the lack of direct information on the later steps of the structural evolution, which precede crystallization. The most natural way to gain an insight into these steps is to consider them as an integral part of a single evolutional process, all steps of which are driven by one and the same force. The later steps of the structural evolution in amorphous alloys are known to follow compositional short-range ordering (SRO), driven by a compound forming tendency, which is typical of all known metallic glasses. If the SRO and the ensuing steps in the structural evolution are actually linked as a single process, which it is reasonable to assume, it immediately follows that the SRO precedes *medium*-range ordering (MRO), which also increases the number of energetically favourable bonds. MRO or, in other words, clustering of associates with a short-range order (formed during the SRO) can involve such steps as the formation of branched chains of associates and a network of these chains. The important point is that a further increase in the number of bonds with strong attractive forces can give rise to an increase in the network density and, as a result, to the formation of small regions depleted of associates, similar to the regions depleted of metalloid atoms and, hence, of associates in the computer simulated structures of transition metal–metalloid alloys [7,8].

* Corresponding author. Tel: +7-096 517 1144. Telefax: +7-096 517 1949. E-mail: stelmukh@issp.ac.ru.

SSDI 0022-3093(95)00452-1

Such regions can, evidently, be regarded as sites at which the nucleation of a primary crystalline phase can occur, when the regions become large enough to allow it. It follows from this consideration that alloying additions enhancing the compound-forming tendency will increase the network stability and, thus, retard the growth of the nucleated crystals and increase the total number of potential nucleation sites converted into viable nuclei during crystallization. Therefore, additions with a strong compound forming ability in a given alloy can be expected to facilitate nanocrystallization [9]. This conclusion is in agreement with the observed effect [3–5] of the addition of boron to Fe- and Co-based alloys containing M elements (M is transition metal: Zr, Nb, Hf) with a strong affinity to boron, as well as with the data on the influence of Nb on the crystallization behaviour of Fe–Cu–Si–B alloys [2,6]. Providing the above consideration is valid, Zr, Nb or Hf additions to boron containing Co-based amorphous alloys, e.g., to Co–Si–B, can be expected to facilitate their nanocrystallization. It was found recently [9] that nanoscale structures are actually formed by crystallization of the a $Co_{78.5}Si_{12.5}B_9$ alloy with 3 wt% Zr. In this work, the crystallization behaviour of the same Co–Si–B alloy is studied, but with Nb and Hf additions.

2. Experimental procedures

3 wt% Nb or Hf were added to 50 g ingots of the $Co_{78.5}Si_{12.5}B_9$ alloy, after which the ingots, together with the additions, were inductively remelted under an argon atmosphere in quartz crucibles. Ribbons of the resulting Co–Si–B–Nb and Co–Si–B–Hf alloys (denoted below as alloy 1 and alloy 2, respectively) 14 mm wide and 16–18 μm thick were prepared by planar flow casting in air onto a steel wheel. The samples were annealed in a tin bath for a short time (up to 60 s) and in a conventional furnace under an argon atmosphere for 3600 s at different temperatures. The short-time annealing was followed by water quenching.

The samples were examined by X-ray diffraction and transmission electron microscopy (TEM). X-ray diffraction θ–2θ scans were performed using monochromated Cu K_α radiation. The samples for the TEM studies were thinned by ion milling. The crystallization behaviour of the as-cast samples during continuous heating at a constant heating rate of 20 K/min was examined by differential scanning calorimetry (DSC) using a Perkin–Elmer DSC7 calorimeter.

3. Results

The results of the DSC measurements are shown in Fig. 1. The first of the exothermic peaks exhibited by each of the alloys is due to the primary crystallization, resulting in the formation of a single hcp crystalline phase in both alloys, as indicated by the diffraction measurements. The lattice parameters of this phase (evaluated from electron diffraction patterns taken from samples of both alloys after primary crystallization under different conditions) are almost the same as those of pure cobalt, which suggests that the phase is a Co-based solid solution. The point which is worthy of note in Fig. 1 is that there are wide temperature intervals between the first and the second peak positions on the DSC curves (132 K for alloy 1 and 119 K for alloy 2). In this respect, the alloys studied are similar to the FMs. (For the well studied $Fe_{73.5}Cu_1Nb_3Si_{13.5}B_9$ FM, this interval was found to be 150 K at a constant heating rate of 10 K/min [6].) The greater the above temperature interval, the wider, apparently, the choice of possibilities to control the primary crystallization in such a way as to avoid the next stage of crystallization. (In the FMs, the secondary crystallization is known to cause structure coarsening and the degradation of the soft magnetic properties of these alloys.)

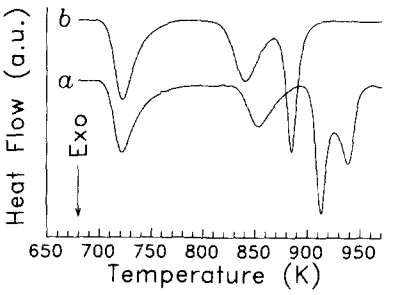

Fig. 1. DSC plots for alloy 1 (a) and alloy 2 (b).

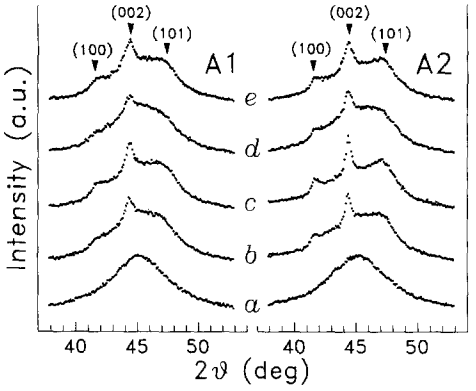

Fig. 2. X-ray diffraction patterns for the samples of alloy 1 (A1) and alloy 2 (A2) in the as-cast state (a) and after annealing at 693 K for 3600 s (b), 733 K for 3600 s (c) and 60 s (d) and at 753 K for 60 s (e).

Fig. 2 shows fragments of the X-ray diffraction patterns for the samples subjected to short-time and conventional furnace annealing at different temperatures. The triangular symbols indicate the positions of the (100), (002) and (101) lines of pure hcp cobalt.

Fig. 3 shows TEM micrographs of the samples of alloy 1 and alloy 2 annealed at 733 K for 3600 s.

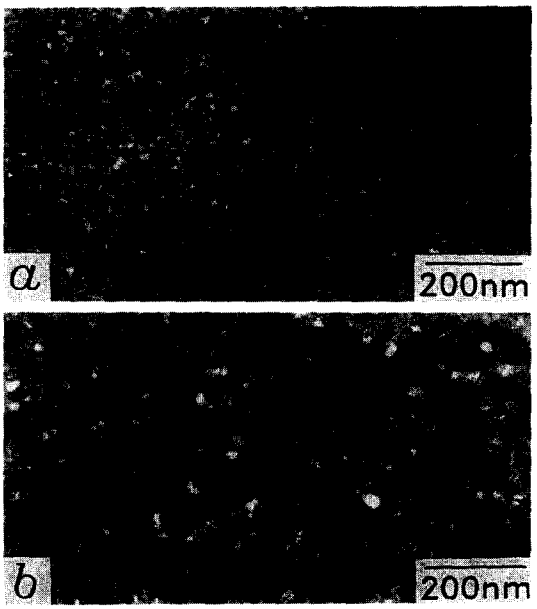

Fig. 3. Bright-field electron micrographs of the samples of alloy 1 (a) and alloy 2 (b) annealed at 733 K for 3600 s.

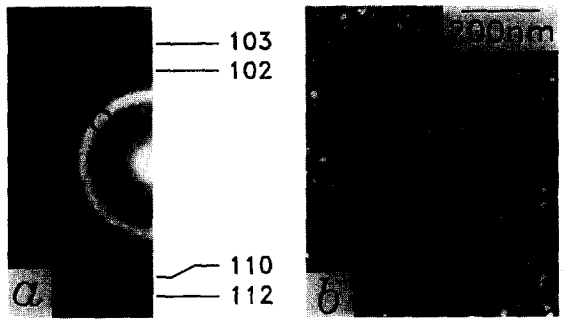

Fig. 4. Electron diffraction pattern (a) and dark-field image (b) for the sample of alloy 1 annealed at 733 K for 3600 s.

The electron diffraction pattern for the sample of alloy 1 annealed at 733 K for 3600 s is shown in Fig. 4(a). The (100), (002) and (101) rings from the hcp phase are overlapped by the amorphous halo. All the rings beyond the amorphous halo were found to come from the hcp phase. Their indices are shown in the figure.

The bright-field images in Fig. 3 show a fine grained structure with grains separated by the remaining amorphous phase. The amorphous phase can be seen highlighted between the grains on the dark-field image in Fig. 4(b), taken with the aperture position represented by the open circle in Fig. 4(a).

The grain size distributions for the samples of alloy 1 and alloy 2, annealed at 753 K for 60 s and at 733 K for 3600 s, are presented in Fig. 5. The

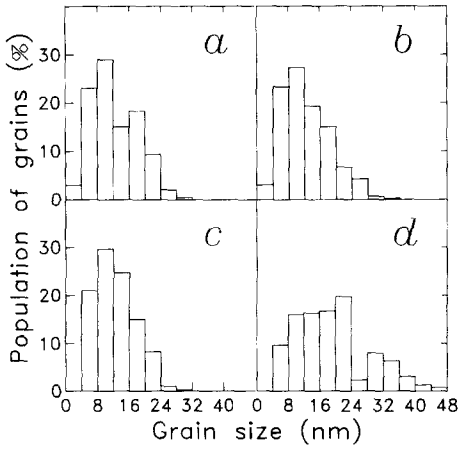

Fig. 5. Grain size distributions in the samples of alloy 1 ((a), (b)) and alloy 2 ((c), (d)) annealed at 753 K for 60 s ((a), (c)) and at 733 K for 3600 s ((b), (d)).

average grain sizes are 12, 13, 13 and 19 nm, as found from the data used to plot grain size distributions (a), (b), (c) and (d), respectively. (About 300 grains were measured to find the average grain size and to plot the grain size distribution.) All of the average values fall within the range characteristic of nanocrystalline materials produced by crystallization of metallic glasses. The difference in the grain size distributions (b) and (d) in Fig. 5 is probably due to the different atomic concentrations of Nb in alloy 1 and Hf in alloy 2. (At the same Nb and Hf weight contents, the Nb atomic concentration is higher than that of Hf.)

The average grain size values found from the TEM measurements agree well with those evaluated from the half-width of the (002) line in the X-ray diffraction patterns, regardless of the fitting procedures used to extract the (002) line contribution to the measured X-ray scattering. It is of interest to note that the widths of the (100), (002) and (101) lines in the reflection spectra shown in Fig. 2 are noticeably different, although the grain shape does not differ too much from equiaxial. The observation suggests a high density of the stacking faults in grains [10].

4. Conclusion

The results of this work show that the medium-range ordering in amorphous alloys can strongly affect their crystallization behaviour. A better understanding of this stage of the structural evolution of metallic glasses can be expected to provide new possibilities for controlling the course of the glass to crystal transformation and the resulting crystalline structure.

The work was supported by the Russian Foundation for Fundamental Research (Project No. 93-02-02213).

References

[1] Y. Yoshizawa, S. Oguma and K. Yamauchi, J. Appl. Phys. 64 (1988) 6044.
[2] Y. Yoshizawa and K. Yamauchi, Mater. Sci. Eng. A133 (1991) 176.
[3] K. Suzuki, N. Kataoka, A. Inoue, A. Makino and T. Masumoto, Mater. Trans. JIM 31 (1990) 743.
[4] K. Suzuki, A. Makino, A. Inoue and T. Masumoto, J. Appl. Phys. 74 (1993) 3316.
[5] H. Kimura, A. Inoue, Y. Murakami and T. Masumoto, Sci. Rep. RITU A-36 (1992) 213.
[6] T. Kulik, Mater. Sci. Eng. A159 (1992) 95.
[7] Ch. Hausleitner and J. Hafner, Phys. Rev. B47 (1993) 5689.
[8] Ch. Hausleitner, J. Hafner and Ch. Becker, Phys. Rev. B48 (1993) 13119.
[9] A. Serebryakov, V. Stelmukh, L. Voropaeva, N. Novokhatskaya, Yu. Levin and A. Gurov, Nanostruct. Mater. 4 (1994) 645.
[10] A.J.C. Wilson, X-ray Optics (Methuen, London, 1949) ch. 6.